9. J. Cortes, S. F. Haydock, G. A. Roberts, D. J. Bevitt, P. F. Leadlay, *Nature* **348**, 176 (1990); D. J. Bevitt, J. Cortes, S. F. Haydock, P. F. Leadlay, *Eur. J. Biochem.* **204**, 39 (1992).
10. P. Caffrey, D. J. Bevitt, J. Staunton, P. F. Leadlay, *FEBS Lett.* **304**, 225 (1992).
11. G. A. Roberts, J. Staunton, P. F. Leadlay, *Eur. J. Biochem.* **214**, 305 (1993).
12. S. J. Wakil, *Biochemistry* **28**, 4523 (1989).
13. A. F. A. Marsden, unpublished data.
14. P. F. Leadlay, *Biochem. J.* **197**, 413 (1981).
15. J. Q. Fuller and P. F. Leadlay, *ibid.* **213**, 643 (1983).
16. J. F. Aparicio, P. Caffrey, A. F. A. Marsden, J. Staunton, P. F. Leadlay, *J. Biol. Chem.*, in press.
17. S. Donadio, J. B. McAlpine, P. J. Sheldon, M. Jackson, L. Katz, *Proc. Natl. Acad. Sci. U.S.A.* **90**, 7119 (1993).
18. J. B. McAlpine *et al.*, *J. Antibiot.* **40**, 1115 (1987).
19. A. R. Fersht, *Enzyme Structure and Mechanism*, (Freeman, New York, ed. 2, 1985), pp. 347–358.
20. D. E. Cane and C.-C. Yang, *J. Am. Chem. Soc.* **109**, 1255 (1987); S. Yue, J. C. Duncan, Y. Yamamoto, C. R. Hutchinson, *ibid.*, p. 1253.
21. B. Sedgwick *et al.*, *Eur. J. Biochem.* **75**, 481 (1977).
22. D. O'Hagan, *Nat. Prod. Rep.* **6**, 205 (1989).
23. Supported by grants from the Science and Engineering Research Council (United Kingdom) (Molecular Recognition Initiative and Biotechnology Directorate–LINK). J.F.A. was the recipient of a European Community bursary. We thank J. R. Knowles and D. A. Hopwood for their comments during preparation of the manuscript.

30 August 1993; accepted 30 November 1993

Rational Design of Potent, Bioavailable, Nonpeptide Cyclic Ureas as HIV Protease Inhibitors

Patrick Y. S. Lam,* Prabhakar K. Jadhav, Charles J. Eyermann, C. Nicholas Hodge, Yu Ru, Lee T. Bacheler, James L. Meek, Michael J. Otto, Marlene M. Rayner, Y. Nancy Wong, Chong-Hwan Chang, Patricia C. Weber, David A. Jackson, Thomas R. Sharpe, Susan Erickson-Viitanen*

Mechanistic information and structure-based design methods have been used to design a series of nonpeptide cyclic ureas that are potent inhibitors of human immunodeficiency virus (HIV) protease and HIV replication. A fundamental feature of these inhibitors is the cyclic urea carbonyl oxygen that mimics the hydrogen-bonding features of a key structural water molecule. The success of the design in both displacing and mimicking the structural water molecule was confirmed by x-ray crystallographic studies. Highly selective, preorganized inhibitors with relatively low molecular weight and high oral bioavailability were synthesized.

Knowledge of the HIV protease (HIV PR) mechanism of action and substrate specificity has been extensively used to design a variety of transition state–based inhibitors with inhibition constants in the nanomolar or subnanomolar range (*1*, *2*). The symmetry of the HIV PR dimer guided the design of twofold (C2) symmetric and pseudosymmetric inhibitors (*3*). However, these inhibitors retain substantial peptide character, and despite many elegant structure-activity studies, it has been difficult to combine adequate potency with oral bioavailability (*3*, *4*). The difficulty in developing such leads into useful therapeutics is challenging, for in addition to the traditional barriers encountered in the drug development process, peptide-based molecules are in general biologically unstable, poorly absorbed, and rapidly metabolized (*5*). This challenge is not unique to HIV PR; transition from peptide-based leads to therapeutics has proven formidable for other enzymes such as renin inhibitors (*6*, *7*).

We have previously explored a series of potent, linear C2-symmetric inhibitors in which the transition state mimetic was a diol (*8*). We were unable to overcome the poor oral bioavailability of these peptide molecules and consequently sought other approaches. The technique of searching databases containing three-dimensional (3D) molecular structures has been used to identify synthetic frameworks that can serve as the starting point for the design of nonpeptide inhibitors, and this approach has been explored with HIV PR. Unfortunately, the HIV PR inhibitors designed to date on the basis of 3D database searches (*9*, *10*) have yielded inhibitors with only micromolar potency.

Our current design of nonpeptide inhibitors (*11*) began with structural information available from published x-ray crystal structures of HIV-PR inhibitor complexes (*12*–*15*). A common feature observed is the presence of a tetracoordinated structural water molecule linking the bound inhibitor to the flexible glycine-rich β strands or "flaps" of the HIV PR dimer (Fig. 1). This water molecule accepts two hydrogen bonds from backbone amide hydrogens of HIV PR residues Ile 50 and Ile 50′ and donates two hydrogen bonds to carbonyl oxygens of the inhibitor, thus inducing the fit of the flaps over the inhibitor (*16*). Its relevance to the generation of HIV PR inhibitors has been noted (*12*, *13*).

We hypothesized that incorporation of the binding features of this structural water molecule into an inhibitor would be beneficial because its displacement should be energetically favorable (*17*). In addition, conversion of a flexible, linear inhibitor into a rigid, cyclic structure with restricted conformations should provide a positive entropic effect. Finally, incorporation of a mimic for the structural water within the inhibitor should ensure specificity for the HIV PR as against other aspartic acid proteases, because this water molecule is unique to retroviral proteases. We reasoned that these effects might provide highly potent and specific binding and reduce the need for multiple interactions at the specificity pockets. This should permit design of smaller (<600 daltons) inhibitors with improved oral bioavailability.

Extensive structure-activity relations (SARs) established for C2-symmetric diols indicated that the diol imparts significant potency as compared with corresponding mono-ol transition state analogs (*3*, *8*). Thus, we wanted to incorporate this feature of the diol–HIV PR interaction into a 3D pharmacophore model. However, no x-ray structure of a C2-symmetric diol-protease complex was available when this work was initiated; two independent reports of structures have since appeared (*18*). Therefore, computer models for C2-symmetric diols bound to the active site of HIV-1 PR were developed from the crystal structure coordinates of a hydroxyethylene inhibitor bound to HIV PR (*15*) by means of distance geometry (*19*) (Fig. 2, A and B) and several pharmacophores were generated.

The simplest pharmacophore model (Fig. 2C) was based on two key intramolecular distances: that between symmetric hydrophobic groups, designated P1 and P1′, that occupy corresponding enzyme pockets S1 and S1′ and that from P1 and P1′ to a hydrogen bond donor/acceptor group (or groups) that binds to catalytic aspartates. A 3D database search (*20*, *21*) with this pharmacophore model yielded the "hit" (*22*) shown in Fig. 2D, which not only met the initial search criteria, but also included an oxygen that matched the structural water found in HIV PR–inhibitor complexes. This 3D search indicated that a phenyl ring could properly position groups to interact with aspartates 25 and 25′ as well as to mimic the structural water (Fig. 2E). However, because a phenyl ring might not properly position all substituents in the

Departments of Virology Research and Chemical and Physical Sciences, The DuPont Merck Pharmaceutical Company, Wilmington, DE 19880.

*To whom correspondence should be addressed.

inhibitor, a cyclohexanone ring (Fig. 2F) was chosen as the initial synthetic scaffold, with the ketonic oxygen as the structural water mimic. The cyclohexanone ring was enlarged to a seven-membered ring (Fig. 2G) to incorporate the diol functionality. This synthetic target was further modified to a cyclic urea (Fig. 2H) on the basis of two considerations. First, cyclic ureas have established a precedent as excellent hydrogen-bond acceptors both in nature [for example, biotin-streptavidin interactions (*23*)] and in synthetic systems (*24*). Second, it was realized that the seven-membered cyclic urea was synthetically accessible by cyclization of the precursor (a phenylalanine-derived diaminodiol) used in the linear C2-symmetric diol series (*8*).

Additional modeling studies were performed with the cyclic ureas to predict the optimal stereochemistry and conformation needed for complementary interaction with the HIV PR. The predicted optimal stereochemistry for cyclic ureas with substituents on the nitrogens is 4*R*, 5*S*, 6*S*, 7*R* (Fig. 2I), which is derived from unnatural (D) phenylalanine. This is in contrast to the linear C2-symmetric diol inhibitors where natural (L) phenylalanine at P1/P1′ provides optimal stereochemistry (*25*). The optimal stereoisomer prefers the conformation with pseudo diaxial benzyl groups and pseudo diequatorial hydroxyl groups (*26*). On the other hand, if the nitrogens of the cyclic ureas are not substituted, enantiomers derived from L- or D-phenylalanine fit equally well at the active site. These conformational preferences were subsequently confirmed by small molecule x-ray crystallography (*27*). Thus, the *N*-substituted cyclic urea ring provides a rigid framework such that with the proper stereochemistry and conformation, the P1/P1′/P2/P2′ and hydroxyls should be highly complementary to the corresponding S1/S1′/S2/S2′ pockets and catalytic aspartates of HIV PR.

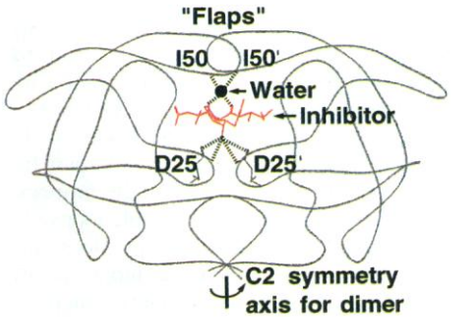

Fig. 1. Key features of the HIV PR dimer. HIV PR is a C2-symmetric dimer, with paired aspartic acid residues located at the floor of the active site and a water molecule juxtapositioned between the inhibitor and flexible enzyme flaps. The complex shown is that of Swain *et al.* (*15*).

That the cyclic urea oxygen is positioned to serve as a surrogate for the structural water molecule in the protease-inhibitor complex is illustrated in the modeled complex shown in Fig. 2J. This model also indicates that the diol functionality should hydrogen bond with both Asp 25 and Asp 25′ of the HIV PR.

While the above design and modeling studies were based on a static, x-ray structural view of the HIV PR active site, the design insights and predictions were confirmed by the biological results and subsequent structural studies. Cyclic ureas derived from L- and D-phenylalanine, when unsubstituted at the urea nitrogens, have essentially identical inhibition constant (K_i) values (3000 nM and 4500 nM, respectively), in agreement with modeling. Nitrogen-substituted analogs of L-phenylalanine–derived cyclic urea do not result in increased potency as compared with the unsubstituted cyclic urea (for example, the *N*,*N*-bis-allyl analog has a K_i of 4500 nM). In contrast, substitution of D-phenylalanine–derived cyclic urea with allyl groups on the nitrogens resulted in cyclic urea **1** (Table 1, K_i = 4.7 nM), which is 1000-fold more potent than the corresponding L-phenylalanine–derived cyclic urea.

There are several factors responsible for the potency of nitrogen-substituted cyclic ureas: (i) the cyclic ureas are preorganized (*28*) for highly complementary binding to HIV PR, with the conformational entropic penalties typically associated with binding a linear, flexible inhibitor being "prepaid" during synthesis rather than during binding; (ii) displacement of the water molecule is probably thermodynamically favorable (*17*); and (iii) hydrophobic interactions between the nitrogen substituents and the S2 and S2′ subsites of HIV PR are optimized with the preferred conformation and stereochemistry.

As part of our discovery program on HIV PR inhibitors, criteria for development of a compound as an oral agent for the treat-

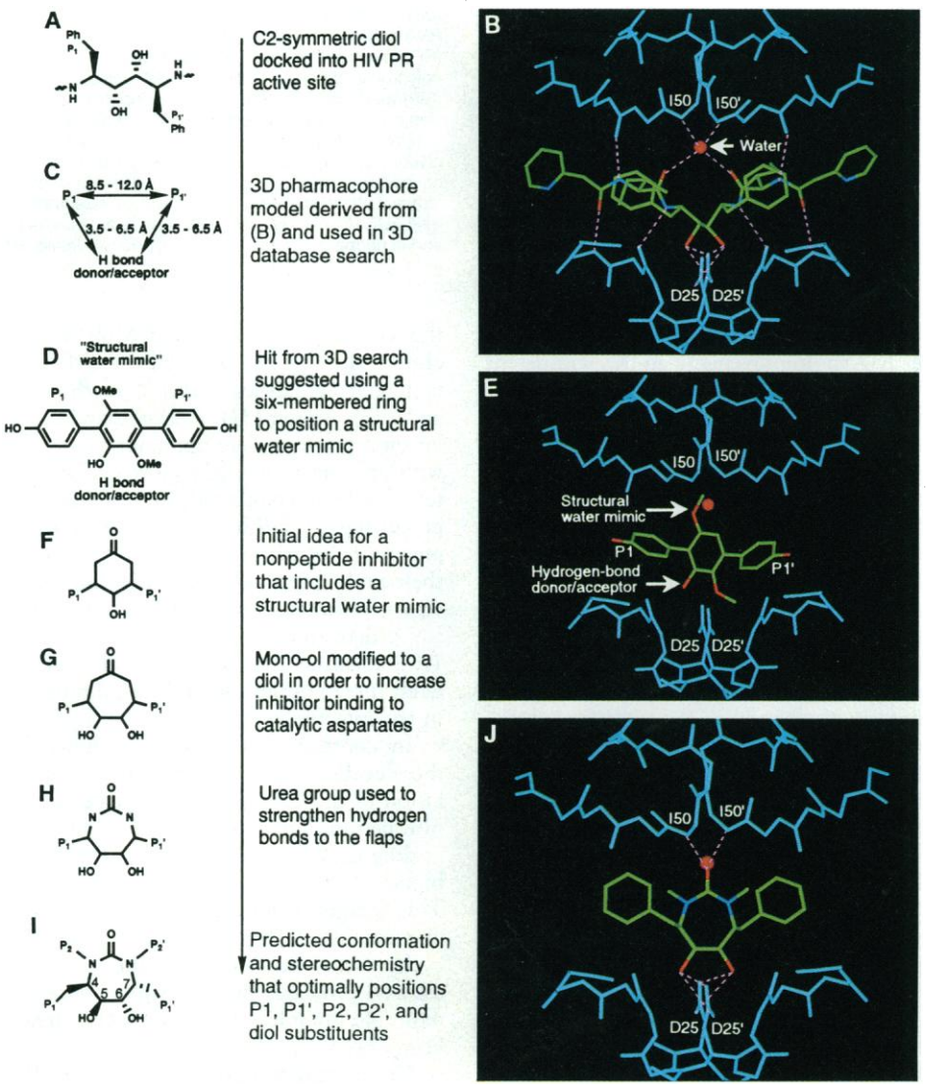

Fig. 2. Strategy and steps involved in the design of cyclic urea inhibitors of HIV PR.

ment of acquired immunodeficiency syndrome (AIDS) were defined. In addition to potency against enzyme and virus in vitro, minimal values were established for the plasma concentrations relative to the antiviral potency for an individual compound after oral dosing. These limits were defined as a peak plasma drug concentration (C_{max}) after oral dosing severalfold higher than the concentration required to inhibit virus replication by 90% (IC_{90}), and a trough concentration with BID (twice a day) or TID (three times a day) dosing greater than or equal to the IC_{90}.

Cyclic urea **1** displays modest antiviral potency (Table 1), as assessed by measurement of viral RNA (*29*) or yield of infectious virus particles (*30*). Although **1** has appreciable oral bioavailability in the rat (*F*% = 49%), doses of 20 mg per kilogram of body weight fail to result in C_{max} concentrations higher than the IC_{90}. Potency against enzyme and virus were improved approximately twofold by replacement of allyl groups with cyclopropylmethyl, **2**. More importantly, **2** has high oral bioavailability in the rat and the dog, such that a dose of 10 mg/kg in the dog results in sustained plasma drug concentrations in excess of the IC_{90}. If the long plasma half-life in the dog (8 hours) is predictive of humans, BID or TID dosing could maintain plasma drug concentrations above the IC_{90}.

Modeling studies revealed that the enzyme's S2/S2′ subsites are relatively large and can accommodate residues such as naphthalene rings. Cyclic urea **3**, containing β-naphthylmethyl substituents, showed a 10-fold improvement in K_i, consistent with an increase in hydrophobic interactions. In this case, however, greater inhibition of enzyme did not result in greater antiviral efficacy, perhaps because the naphthyl substituents are too lipophilic. Additional modeling studies suggested that introduction of hydrogen-bonding groups on otherwise lipophilic urea nitrogen substituents might further increase S2/S2′ subsite affinity and provide greater antiviral efficacy.

Cyclic urea **4**, which incorporates *p*-hydroxymethylbenzyl as the nitrogen substituent, combines good potency against virus and HIV PR with significant oral bioavailability (Table 1). In the rat and the dog, plasma drug concentrations severalfold higher than the antiviral IC_{90} are achieved. Because of the combination of high potency and significant bioavailability, compound **4**, designated DMP 323, is currently undergoing additional study, including phase I clinical investigation.

To demonstrate that the antiviral activity of cyclic ureas reflects inhibition of HIV-1 PR, we assessed the ability of cyclic ureas **1** through **4** to inhibit processing of the viral *gag* polyprotein in Molt 4 cells chronically infected with HIV-1 (RF) and metabolically labeled with [^{35}S]methionine and [^{35}S]cysteine (*31*). Released and cellular viral proteins were immunoprecipitated with antisera to gag p24 protein. The potency of these compounds in inhibiting the processing of full-length *gag* polyprotein precursor to mature p24 closely mirrors their rank order and potency in inhibiting virus replication as measured by either viral RNA detection or yield reduction (Table 1), indicating that the antiviral effect is likely due to inhibition of the viral protease in the infected cells.

In contrast to the potency shown by these cyclic ureas toward HIV PR, no inhibition of the cellular aspartyl proteases renin, pepsin, and cathepsin D was observed at drug concentrations at least 3000 times higher than the K_i value for HIV-1 PR. This specificity for HIV-1 PR is a consequence, at least in part, of the design of the cyclic ureas, since only in the retroviral aspartyl proteases has the structural water molecule (mimicked by the cyclic ureas) been observed.

Crystal structures of 10 cyclic urea–HIV PR complexes have been determined. The structure of compound **3**–HIV PR complex (*32*) is presented here since it is currently of the highest resolution (1.8 Å) and refinement (final *R* factor = 19.5%). Inspection of electron density maps shows the conformation of the inhibitor bound at the protease active site and reveals that the diad symmetry axes of the inhibitor and protease are nearly coincident. As shown in Fig. 3, the inhibitor is situated with the seven-membered ring roughly perpendicular to the plane of the catalytic aspartates. Both inhibitor diol oxygens are positioned to interact with these carboxylates. The carbonyl oxygen of the inhibitor accepts hydrogen bonds from backbone amides of Ile 50 and its symmetry-related counterpart Ile 50′. Thus, the inhibitor links the protease catalytic aspartates to the flexible loops via a hydrogen bond network that does not include an intervening water molecule, in contrast to what is seen in x-ray structures of HIV-1 PR complexed with linear peptidomimetic inhibitors (*12–16, 18*).

The issues of preclinical efficacy assessment and development of resistance to HIV therapeutics are of special interest for AIDS therapeutics. The lack of reliable small animal models for AIDS has hampered the

Table 1. Biological properties of cyclic urea inhibitors of HIV protease (*37*).

Parameter	1	2	3	4
Compound	1	2	3	4
Molecular weight	407	435	607	567
K_i* (nM)	4.7 ± 0.3	2.14 ± 0.52	0.31 ± 0.06	0.27 ± 0.05
IC_{50}* (μM)	0.63	0.30	0.22	0.036
IC_{90} RNA† (μM)	4.70 ± 2.68	1.75 ± 0.73	3.86 ± 1.3	0.057 ± 0.028
IC_{90} YIELD‡ (μM)	3.69 ± 0.49	1.83 ± 0.22	ND	0.119 ± 0.035
IC_{90} RIP§ (μM)	11.82	3.91	1.65	0.160
TC_{50}‖ (μM)	93.1 ± 15.9	33.6 ± 9.9	14.8 ± 6.2	61.5 ± 10.4
		Rat bioavailability¶		
PO dose (mg/kg)	20	10	20	10
C_{max} (μM)	2.70	4.34	0.38	0.78
$t_{1/2}$ (hours)	1.1	1.1	ND	1.5
F%	49 ± 32	100 ± 28	ND	27 ± 7
		Dog bioavailability¶		
PO dose (mg/kg)	ND	10	ND	5
C_{max} (μM)		9.24		1.56
$t_{1/2}$ (hours)		8.0		1.08
F%		48 ± 14		37 ± 19

*K_i values were measured as described (*38*), with 62.5 to 250 pM HIV PR dimer and 1 to 10 nM inhibitor. The concentration giving 50% inhibition of cleavage of gag polyprotein precursor was measured as described (*38*). †Inhibition of viral replication was quantified in HIV-1 (RF)–infected MT2 cells by measurement of viral RNA with an oligonucleotide-based sandwich hybridization assay (*29*). ‡Inhibition of viral replication in HIV-1 (RF)–infected MT2 cells was quantified by a yield reduction assay as described (*30*). §Inhibition of gag polyprotein processing in chronically infected Molt4 cells was determined by radioimmunoprecipitation assay (RIP) as described (*31*). ‖The concentration of compound that produced a 50% reduction in the number of viable cells as determined by metabolism of a tetrazolium dye was designated the TC_{50}. ¶Bioavailability was determined in groups of rats or dogs (n = 4 per group) dosed with compound in formulations containing propylene glycol, polyethylene glycol 400, water. The maximum plasma concentration (C_{max}) is the observed peak plasma concentration after an oral dose. The plasma elimination half-life, $t_{1/2}$, was determined by linear regression of the terminal phase of the logarithm plasma concentration–time curve. Oral bioavailability (*F*%) was determined by the ratio AUC PO/AUC IV, where AUC is the area under the plasma concentration–time curve from time zero to infinity and is normalized for dose. ND, not done. Details will be published elsewhere.

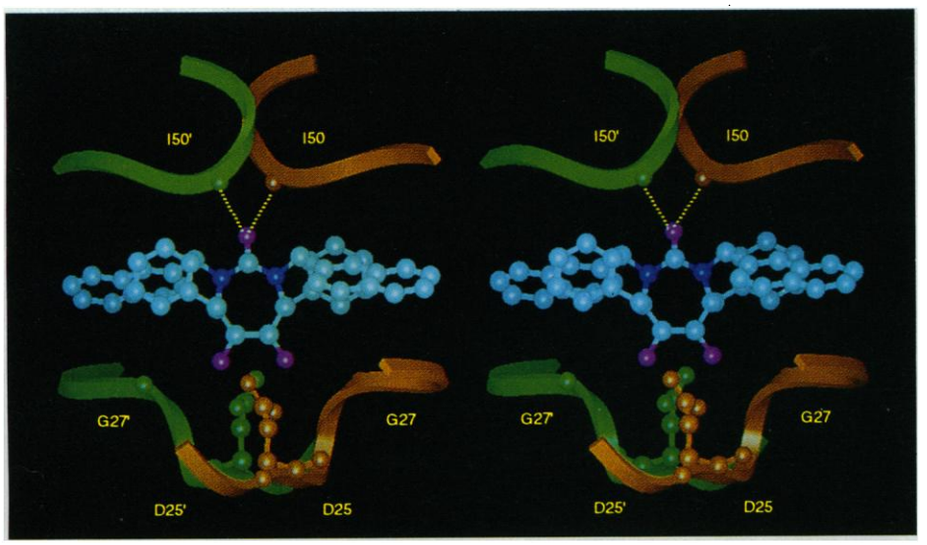

Fig. 3. Stereo drawing of the inhibitor in the active site of HIV-1 PR (*32*). All heavy atoms of the inhibitor are shown in ball and stick representation, and a selected portion of the protein backbone as a ribbon—brown for the monomer 1 and green for monomer 2. The active site aspartic acids Asp 25 and 25′, the backbone carbonyl oxygens of Gly 27 and Gly 27′, and the amino nitrogen atoms of Ile 50 and Ile 50′ are shown as solid spheres. Colors used for the inhibitor are gray for carbon, blue for nitrogen, and pink for oxygen. The phenyl and naphthyl rings of the inhibitor pack in the hydrophobic S1/S1′ and S2/S2′ pockets, respectively.

drug discovery process in that in vivo efficacy testing cannot be easily assessed during preclinical studies. Rodent models that mimic in some way the HIV infection process, or are based on expression of a component (or components) of the HIV genome are currently an active area of research [for example, the use of transgenic mice or Friend leukemia virus models (*33*)]. Preliminary results with a transgenic mouse line in which cataracts develop as a result of the expression of HIV PR under control of the lens α-crystalline promoter indicates that DMP 323 (cyclic urea **4**) causes a delay in the appearance of these HIV PR–dependent cataracts (*34*). The limited efficacy against SIV_{mac} (IC_{90} = 0.90 μM) suggests that the simian immunodeficiency virus–rhesus monkey model may not be a useful animal model in which to evaluate this compound. Recent clinical findings and in vitro studies suggest that the utility of some inhibitors of another HIV target, the reverse transcriptase, may be limited because of rapid onset of resistance to therapeutic agents through target mutation (*35*). Studies in progress with DMP 323 suggest that mutations within the HIV PR leading to resistance occur only after prolonged passage in culture and lead to increases in the apparent IC_{90} of less than 10-fold (*36*). Further studies will map the extent and multiplicity of mutations in the HIV PR gene selected by growth in the presence of cyclic ureas. Use of structure-based design techniques should promote the development of improved compounds with activity against both wild-type and mutant HIV PR.

REFERENCES AND NOTES

1. T. L. Blundell *et al.*, *Trends Biochem. Sci.* **15**, 425 (1990); D. W. Norbeck and D. J. Kempf, *Annu. Rep. Med. Chem.* **26**, 141 (1991); A. G. Tomasselli *et al.*, *Chim. Oggi*, 6 (1991); C. Debouck, *AIDS Res. Hum. Retroviruses* **8**, 153 (1992); J. A. Martin, *Antiviral Res.* **17**, 265 (1992); R. Yarchoan, H. Mitsuya, S. Broder, *Trends Pharmacol. Sci.* **14**, 196 (1993).
2. R. E. Babine *et al.*, *Bioorg. Med. Chem. Lett.* **2**, 541 (1992); S. Ikeda, J. A. Askley, P. Winsching, K. D. Janda, *J. Am. Chem. Soc.* **114**, 7604 (1992); D. H. Rich *et al.*, *J. Med. Chem.* **35**, 3803 (1992); A. K. Ghosh *et al.*, *ibid.* **36**, 292 (1993); D. P. Getman *et al.*, *ibid.*, p. 288; W. J. Thompson *et al.*, *J. Am. Chem. Soc.* **115**, 801 (1993); D. S. Holmes *et al.*, *Bioorg. Med. Chem. Lett.* **3**, 503 (1993).
3. D. J. Kempf *et al.*, *J. Med. Chem.* **36**, 320 (1993).
4. G. J. Muirhead *et al.*, *Proceedings of the British Pharmacological Society* (1992), p. 170; P. E. O. Williams, G. J. Muirhead, M. J. Madigan, A. M. Mitchell, T. Shaw, *ibid.*, p. 156; T. M. Shaw, G. J. Muirhead, N. Parish, G. R. McClelland, A. C. Houston, *ibid.*, p. 167.
5. J. J. Plattner and D. W. Norbeck, in *Drug Discovery Technologies*, C. R. Clark and W. H. Moos, Eds. (Ellis Horwood, Chichester, England, 1990), pp. 92–126.
6. W. J. Greenlee, *Med. Res. Rev.* **10**, 173 (1990); S. H. Rosenberg *et al.*, *J. Med. Chem.* **36**, 449 (1993).
7. H. D. Kleinert *et al.*, *Science* **257**, 1940 (1992).
8. P. K. Jadhav, L. R. McGee, A. Shenvi, C. N. Hodge, PCT Patent Application WO 91/18 866A (1991); P. K. Jadhay, F. J. Woerner, *Bioorg. Med. Chem. Lett.* **2**, 353 (1992); M. J. Otto *et al.*, *VIIIth Int. Conf. AIDS Amsterdam* 1, 203 (1992).
9. I. D. Kuntz, J. M. Blaney, S. J. Oatley, R. Langridge, T. E. Ferrin, *J. Mol. Biol.* **161**, 269 (1982); R. L. DesJarlais *et al.*, *Proc. Natl. Acad. Sci. U.S.A.* **87**, 6644 (1990).
10. J. H. VanDrie, D. Weininger, Y. C. Martin, *J. Comput.-Aided Mol. Des.* **3**, 225 (1989); M. G. Bures *et al.*, *Tetrahedron Comput. Methodol.* **3**, 673 (1990).
11. P. Y. S. Lam, C. J. Eyermann, C. N. Hodge, P. K. Jadhav, G. V. Delucca, PCT Patent Application WO 9307128 (1993). Patent also includes five- and six-membered ring cyclic ureas that have been synthesized and found to be active. Other cycles capable of displacing the structural water can be envisioned, for example, cyclic cyanoguanidines.
12. A. Wlodawer *et al.*, *Science* **245**, 616 (1989).
13. J. Erickson *et al.*, *ibid.* **249**, 527 (1990).
14. R. Lapatto *et al.*, *Nature* **342**, 299 (1989); M. Miller *et al.*, *Science* **246**, 1149 (1989); P. M. D. Fitzgerald *et al.*, *J. Biol. Chem.* **265**, 14209 (1990); M. Jaskolski *et al.*, *Biochemistry* **30**, 1600 (1991); G. Dreyer *et al.*, *ibid.* **31**, 6646 (1992); T. J. Tucker *et al.*, *J. Med. Chem.* **35**, 2525 (1992); R. Bone, J. Vacca, P. S. Anderson, M. K. Holloway, *J. Am. Chem. Soc.* **113**, 9382 (1992). For a review of HIV PR crystallography, see A. Wlodawer and J. Erickson [*Annu. Rev. Biochem.* **62**, 543 (1993)].
15. A. L. Swain *et al.*, *Proc. Natl. Acad. Sci. U.S.A.* **87**, 8805 (1990).
16. A. Gutschina, I. T. Weber, *FEBS Lett.* **269**, 269 (1990).
17. S. N. Timasheff, *Biochemistry* **31**, 9857 (1992).
18. G. B. Dreyer *et al.*, *ibid.* **32**, 937 (1993); N. Thanki *et al.*, *Protein Sci.* **1**, 1061 (1992).
19. J. M. Blaney, G. M. Crippen, A. Dearing, J. S. Dixon, DGEOM, Quantum Chemistry Program Exchange 590.
20. W. C. Ripka and C. J. Eyermann, in *Proceedings of the 2nd International Conference on Chemical Information*, W. Warr, Ed. (Springer-Verlag, Heidelberg, Germany, 1993, pp. 303–314); for a review, see Y. C. Martin [*J. Med. Chem.* **35**, 2145 (1992)].
21. Three-dimensional (3D) searches were done on a subset of the Cambridge Structural Database (see Allen, below) that has been converted for use with MACCS-3D. C. J. Eyermann, unpublished results; F. H. Allen *et al.*, *J. Chem. Inf. Comput. Sci.* **31**, 187 (1991); MACCS-3D, Molecular Design Limited, San Leandro, CA.
22. G. D. Andreetti, G. Bocelli, P. Sgarabotto, *Cryst. Struct. Commun.* **3**, 145 (1974).
23. P. C. Weber, D. H. Ohlendorf, J. J. Wendoloski, F. R. Salemme, *Science* **243**, 85 (1989).
24. D. J. Cram and P. Y. S. Lam, *Tetrahedron* **42**, 1607 (1986); D. J. Cram, I. B. Dicker, M. Lauer, C. B. Knobler, K. N. Trueblood, *J. Am. Chem. Soc.* **106**, 7150 (1984).
25. P. Y. S. Lam and P. K. Jadhav, unpublished observations.
26. Since seven-membered cyclic ureas can exist in two possible psuedo chair conformations, a conformational analysis was conducted. When the nitrogens are unsubstituted, 1,3-diaxial strain dominates, and the conformer with pseudo diequatorial benzyl groups and pseudo diaxial hydroxyl groups is preferred [J. March, *Advanced Organic Chemistry* (Wiley, New York, ed. 3, 1985), p. 125]. In contrast, when the two nitrogens are substituted with P2/P2′ groups, the converse is true. The partial double bond character of the urea C-N bond introduces severe allylic 1,2 strain [F. Johnson, *Chem. Rev.* **68**, 375 (1968)] between the benzyl groups and the nitrogen substituents. This allylic 1,2-strain overcomes the 1,3-diaxial strain, and the conformer with pseudo diaxial benzyl groups and pseudo diequatorial hydroxyl groups is preferred.
27. J. C. Calabrese, P. Y. S. Lam, G. V. Delucca, unpublished observations.
28. D. J. Cram, *Science* **240**, 760 (1988); ——— and G. M. Lein, *J. Am. Chem. Soc.* **107**, 3657 (1985).
29. L. Bacheler *et al.*, *Antiviral Chem. Chemother.*, in press.
30. J. M. Smallheer *et al.*, *ibid.* **4**, 27 (1993).
31. H. Schatzl, H. R. Gelderblom, H. Nitschko, K. von der Helm, *Arch. Virol.* **120**, 71 (1991); M. Rayner *et al.*, in preparation.
32. Purified recombinant HIV PR mixed with excess of inhibitor was crystallized at pH 5.4; conditions used were similar to those previously reported (*13*). Hexagonal rods (0.12 by 0.10 by 0.35 mm, space group $P6_1$, $a = b$ = 62.8 Å, c = 83.5 Å) grew within several days. Diffraction data were collected in 2° oscillation images exposed for 50 min; an R-AXIS imaging plate with an 82-mm

crystal-to-detector distance was used. Intensities for 15,417 unique reflections representing 94% of possible data to 1.8 Å resolution were obtained from 55,263 independent measurements taken on 21 images (R_{sym} = 0.061). The initial *R* factor was 0.40. After crystallographic refinement by simulated annealing [A. Brunger, J. Kuriyan, M. Karplus, *Science* **235**, 458 (1987)], the *R* factor had dropped to 0.26, and electron density maps calculated at this stage revealed the bound conformation of cyclic urea **3**. Geometric refinement parameters for the inhibitor were derived from its single-crystal structure (the crystal structure of **3** alone was determined by J. Calabrese). The final *R* factor was 0.195 for 12,695 reflections to 1.8 Å resolution for which $F \geq 2$ s (*F*). Coordinates will be deposited in the Brookhaven Data Bank [F. Bernstein *et al.*, *J. Mol. Biol.* **112**, 535 (1977)], and additional details will be published elsewhere.

33. Y. Iwakura *et al.*, *AIDS* **6**, 1069 (1992). M-H T. Lai *et al.*, *J. Acq. Immune Defic. Syndr.* **6**, 24 (1993).
34. G. Jonak *et al.*, unpublished observations.
35. T. J. Dueweke *et al.*, *Proc. Natl. Acad. Sci. U.S.A.* **90**, 4713 (1993); M. Tisdale, S. D. Kemp, N. R. Parry, B. A. Larder, *ibid.*, p. 5633.
36. M. J. Otto *et al.*, paper presented at the 2nd International Workshop on HIV Drug Resistance, Noordwijk, The Netherlands, 3 to 5 June 1993.
37. All compounds reported here have satisfactory spectroscopic and elemental analysis.
38. K_i values were determined with recombinant single-chain dimeric HIV protease and a fluorescent substrate [described by Y. S. E. Cheng *et al.*, *Proc. Natl. Acad. Sci. U.S.A.* **87**, 9660 (1990)]. The use of single-chain dimeric protease allows enzyme concentrations as low as 0.0625 nM to be used. Reaction products were separated by high-performance liquid chromatography with a Pharmacia Mono Q anion-exchange column, and the product was quantified by fluorescence. The ability of test compounds to block cleavage of the HIV-1 gag polyprotein was assessed with [^{35}S]methionine-labeled in vitro translation product corresponding to *gag* p17 plus the first 78 amino acids of *gag* p24 and recombinant HIV PR as described [S. Erickson-Viitanen *et al.*, *AIDS Res. Hum. Retroviruses* **5**, 577 (1989)]. Cyclic ureas such as compound **1** and **4** were found to be competitive inhibitors of HIV PR.
39. We are grateful to the HIV protease inhibitors team at The DuPont Merck Pharmaceutical Co. for their hard work and support. We thank A. Wlodawer for providing coordinates of several HIV-1 protease inhibitor complexes.

6 April 1993; accepted 19 October 1993

Regulation of MHC Class I Transport by the Molecular Chaperone, Calnexin (p88, IP90)

Michael R. Jackson, Myrna F. Cohen-Doyle, Per A. Peterson, David B. Williams*

Assembled class I histocompatibility molecules, consisting of heavy chain, β_2-microglobulin, and peptide ligand, are transported rapidly to the cell surface. In contrast, the intracellular transport of free heavy chains or peptide-deficient heavy chain–β_2-microglobulin heterodimers is impaired. A 90-kilodalton membrane-bound chaperone of the endoplasmic reticulum (ER), termed calnexin, associates quantitatively with newly synthesized class I heavy chains, but the functions of calnexin in this interaction are unknown. Class I subunits were expressed alone or in combination with calnexin in *Drosophila melanogaster* cells. Calnexin retarded the intracellular transport of both peptide-deficient heavy chain–β_2-microglobulin heterodimers and free heavy chains. Calnexin also impeded the rapid intracellular degradation of free heavy chains. The ability of calnexin to protect and retain class I assembly intermediates is likely to contribute to the efficient intracellular formation of class I–peptide complexes.

Class I molecules of the major histocompatibility complex (MHC) present peptides derived from endogenously synthesized proteins to cytotoxic T cells. Assembly of the class I heavy chain with β_2-microglobulin (β_2m) occurs rapidly within the ER (*1*, *2*). Peptides arising from protein degradation within the cytosol are delivered to assembling class I molecules by transporter proteins (TAP1 and TAP2) localized to membranes of the ER and *cis*-Golgi (*3*, *4*). For most class I molecules, transport to the cell surface is rapid, although allotype-specific variation is observed in the rate of transport from the ER to the Golgi apparatus (Table 1, mouse lymphoma). In murine RMA-S cells, which have a mutation in the TAP2 protein (*5*), K^b and D^b heavy chains associate with β_2m (*6*, *7*) but are largely deficient in peptide ligand (*8*–*11*) and are transported from the ER to Golgi very slowly (Table 1, RMA-S). Peptide-deficient class I molecules can also be produced by expression of murine heavy chains and β_2m in *Drosophila* Schneider cells because these cells lack auxiliary proteins required for supplying peptides to assembling class I molecules (*12*). The peptide-deficient class I molecules synthesized by *Drosophila* cells are transported much more rapidly than their counterparts in RMA-S cells. Peptide-deficient D^b, K^b, and L^d heterodimers in *Drosophila* cells acquired resistance to digestion by endoglycosidase H (reflective of transport through the Golgi) with half-times of 25, 60, and 80 min, respectively, as compared to >180 and 100 min for D^b and K^b heterodimers in RMA-S (Table 1). These findings suggested that a mechanism exists in mammalian cells for retaining incompletely assembled class I molecules, a mechanism that is nonexistent or impaired in *Drosophila*.

Calnexin is a membrane-bound chaperone of the ER that interacts transiently with a diverse array of wild-type proteins at early stages in their synthesis and in a prolonged fashion with misfolded or incompletely assembled proteins (*1*, *6*, *13*–*18*). As yet, there have been no direct demonstrations of the functions that calnexin may serve in these interactions. Because calnexin binds quantitatively to newly synthesized class I heavy chains in mouse cells (*1*), we assessed its ability to influence the transport of incompletely assembled class I molecules in *Drosophila* cells. Stably transfected *Drosophila* cell lines were prepared that expressed murine K^b, D^b, or L^d heavy chains with or without β_2m in the absence or presence of calnexin (*19*). A protein immunoblot of lysates from these transfectants revealed that cells transfected with the calnexin complementary DNA (cDNA) expressed calnexin in amounts comparable to those observed in murine tumor cells, whereas cells lacking this cDNA exhibited only trace amounts of two endogenous proteins of ~90 kD (Fig. 1). Thus, *Drosophila* cells either do not possess substantial amounts of a calnexin homolog or the similarity in structure is not sufficient to permit cross-reactivity with antibodies to calnexin.

Expression of calnexin slowed ER to Golgi transport of peptide-deficient D^b-β_2m heterodimers from a half-time ($t_{1/2}$) of 25 to 125 min (Fig. 2A). In cells lacking calnexin, the intensity of the heavy chain band increased after prolonged periods of time. This was due to slow assembly of the D^b heavy chain with β_2m, an event that was required for immunoreactivity (*20*). In cells expressing calnexin, assembly occurred much more rapidly, suggesting that calnexin may promote assembly of the D^b heavy chain with β_2m in addition to slowing the transport of the heterodimer. To confirm that a complex was indeed formed between peptide-deficient D^b-β_2m heterodimers and calnexin, we performed a comparable pulse-chase experiment, except that cells were lysed in the presence of the homobifunctional cross-linker DSP. In cells lacking calnexin, the only cross-linked species recovered had an apparent molecular size of ~60 kD (Fig. 2B). However, in cells expressing calnexin, other cross-linked species were observed as a doublet of ~170 kD

M. R. Jackson and P. A. Peterson, Department of Immunology, The Scripps Research Institute, La Jolla, CA 92037.
M. F. Cohen-Doyle and D. B. Williams, Department of Biochemistry, Medical Sciences Building, University of Toronto, Toronto, Ontario M5S 1A8, Canada.
*To whom correspondence should be addressed.